Hindawi
Mobile Information Systems
Volume 2021, Article ID 1362640, 8 pages
https://doi.org/10.1155/2021/1362640

Research Article

A Novel Sparse Array Configuration with Low Coarray Redundancy for DOA Estimation in Mobile Wireless Sensor Network

Pin-Jiao Zhao,[1] **Guo-Bing Hu**,[1] **and Liang-Tian Wan**[2]

[1]*Department of Electronic and Information Engineering, Jinling Institute of Technology, Nanjing 211169, China*
[2]*Key Laboratory for Ubiquitous Network and Service Software of Liaoning Province, School of Software, Dalian University of Technology, Dalian 116620, China*

Correspondence should be addressed to Pin-Jiao Zhao; zhaopinjiao@hrbeu.edu.cn

Received 24 September 2021; Accepted 25 October 2021; Published 22 November 2021

Academic Editor: Lingwei Xu

For tacking and localizing sources in the mobile wireless sensor network, underdetermined direction of arrival (DOA) estimation with high-accuracy is a crucial issue. In this paper, a novel sparse array configuration is developed for accurate DOA estimation from the perspective of sum-difference coarray (SDCA). As compared with most of the existing sparse array configurations, the proposed array can effectively reduce the overlap between difference coarray (DCA) and sum coarray (SCA) and can achieve more consecutive degrees of freedom (DOF), more sources can be resolved accordingly. Additionally, the proposed array has hole-free DCA and SDCA. Then, the concept of coarray redundancy ratio (CRR) is introduced for evaluating the coarray overlap quantitatively and the closed-form CRR expressions of the proposed array are derived in detail. Based on the good properties of the proposed array, vectorized conjugate augmented MUSIC (VCAM) is adopted for underdetermined DOA estimation. The theoretical propositions and numerical simulations demonstrate the superior performance of the proposed array in terms of CRR, consecutive DOF, and DOA estimation accuracy.

1. Introduction

In the large-scale mobile wireless communication network [1, 2], underdetermined direction of arrival (DOA) estimation [3–6] with high-accuracy is a key issue to solve for tacking and localizing sources. The optimized array configuration design is a prerequisite for accurate DOA estimation. Recently, the emerging sparse arrays break through the constraint of spatial sampling theorem by sparsely arranging the array elements and have remarkable advantages in array element layout flexibility, degrees of freedom (DOF), and virtual array aperture [7, 8]. Benefiting from the sparse arrays, more sources than the number of the physical sensors can be resolved with high-accuracy.

From the view of array configuration design, coprime array (CPA) [9] and nested array (NA) [10] are the two most typical sparse arrays. In comparison to the minimum redundancy array and the minimum hole array, CPA and NA are easy to construct since their sensor locations are analytically tractable. Specifically, CPA is obtained from a pair of coprime uniform linear arrays (ULA), which can offer $O(MN)$ DOF with $O(M+N)$ sensors, but has holes in the virtual coarray. By contrast, NA contains two "nesting" ULAs with increasing element spacing, which has a consecutive virtual coarray with $O(N^2)$ DOF from $O(N)$ sensors. On the basis of these prototypes, several modifications are developed, such as generalized CPA [11], thinned CPA [12], super NA [13], and augmented NA [14], aiming at increasing consecutive DOF and expanding effective array aperture. Nevertheless, note that these arrays construct synthetic virtual arrays from the view of difference coarray (DCA), the number of consecutive DOF in the virtual array cannot be more than twice of the physical aperture. Accordingly, the number of the resolvable sources and the DOA estimation accuracy are also affected.

Alternatively, several array configurations based on sum-difference coarray (SDCA) have attracted considerable interests, wherein the introduction of sum coarray (SCA) originating from multiple-input multiple-output (MIMO) system [15, 16] can bring more DOF. In [17], a novel CPA based on SDCA is presented, from which the consecutive DOF more than twice of array aperture can be obtained. Following this, a modified nested array configuration named as sum-diff NA (SdNA) is proposed in [18]. To further improve the available DOF, two kinds of improved NAs [19], termed as INAwSDCA-I and INAwSDCA-II, are developed by rearranging the translational NA. In [20], the unfold CPA configuration with SDCA is proposed. However, for the above array configurations based on SDCA, lots of overlapping virtual sensors between their DCA and SCA lead to unsatisfactory coarray utilization. In addition, there also exist holes in the SDCA. Toward this end, transformed NA (TNA) is designed in [21], which can reduce the overlap between DCA and SCA to some extent, but the degree of overlap under different number of array elements is only evaluated via simulations, lacking quantificational analysis.

To tackle these problems, a novel sparse array configuration with low coarray overlap is proposed in this paper. The proposed array is constructed with two concatenated subarrays with different interelement spacings. From the perspective of virtual array, both the DCA and SDCA of the proposed array are hole-free and can provide more consecutive DOF accordingly. Moreover, the coarray redundancy ratio (CRR) of the proposed array is derived in detail to evaluate the coarray overlap quantitatively. Based on the proposed array, the vectorized conjugate augmented MUSIC (VCAM) approach can be employed for DOA estimation. Now, we briefly summarize the contributions of this work as follows:

(1) A novel array configuration is proposed to reduce the overlap between DCA and SCA

(2) The proposed array has hole-free DCA and SDCA, which has been proved via theoretical propositions

(3) More sources than twice of the number of sensors can be resolved

The mathematical notations used throughout this paper are denoted as follows. Vectors and matrices are denoted by lowercase and uppercase bold-face letters, respectively. $(\cdot)^T$, $(\cdot)^H$, and $(\cdot)^*$ denote transpose, conjugate transpose, and conjugate. $E[\cdot]$ and $|\cdot|$ represent the statistical expectation and modulus of the internal entity, $\partial f(a)/\partial a$ denotes the derivation of $f(a)$ with respect to a, $\mathbf{Z}$ denotes the non-negative integer set, $\mathbf{Z}^+$ denotes the positive integer set, $\mathbf{Z}(n)$ denotes a set of consecutive positive integers ranging from 1 to n in the case of $n > 0$, and $\complement(n) = \{0\}$ holds in the case of $n = 0$; otherwise, $\complement(n)$ denotes a set of consecutive negative integers ranging from $-n$ to -1. The symbol $\otimes$ denotes the Kronecker product and $\odot$ denotes the Khatri–Rao product.

The remainder of this paper is organized as follows. The DOA estimation model based on SDCA is formulated in Section 2. Section 3 presents the proposed low coarray redundancy array configuration in detail. Section 4 exhibits the simulation results in terms of CRR, consecutive DOF, and DOA estimation accuracy. Conclusions are drawn in Section 5. The proofs of Propositions 1 and 2 are derived in Appendix A and Appendix B.

2. Problem Formulation

Assume that K far-field narrowband sources from directions $\{\theta_k | k = 1, 2, \ldots, K\}$ impinge on an N-element nonuniform sparse antenna array. Then, the array output at time t can be represented as

$$\mathbf{x}(t) = \mathbf{A}\mathbf{s}(t) + \mathbf{n}(t) = \sum_{k=1}^{K} \mathbf{a}(\theta_k)\mathbf{s}_k(t) + \mathbf{n}(t), \tag{1}$$

where the value of K is known in advance which can be estimated via source number estimation methods [22]. $\mathbf{s}(t) = [s_1(t), s_2(t), \ldots, s_K(t)]^T$ is the source vector with the kth element being $s_k(t) = G_k e^{jw_k t}$, G_k is the deterministic complex amplitude, and w_k is the frequency offset. $\mathbf{A} = [\mathbf{a}(\theta_1), \mathbf{a}(\theta_2), \ldots, \mathbf{a}(\theta_K)]$ denotes the array manifold matrix. After normalizing by the unit element spacing d, the steering vector can be expressed as $\mathbf{a}(\theta_k) = e^{-j\mathbf{g}\pi \sin\theta_k}$ with $\mathbf{g} = [g_1, g_2, \ldots, g_N]^T$ being the sensor location vector. $\mathbf{n}(t)$ is the Gaussian white noise vector with zero mean and variance being σ_n^2. By collecting T_s samples, the time average function can be expressed as

$$R_{x_i^* x_j}(\tau) = \frac{1}{T_s}\sum_{t=1}^{T_s} x_i^*(t)x_j(t+\tau) \approx \sum_{k=1}^{K} e^{j\pi(g_j - g_i)\sin\theta_k} R_{s_k^* s_k}(\tau) + R_{n_i^* n_j}(\tau), \tag{2}$$

where $\tau \neq 0$ is the time lag, $x_i(t)$ and $x_j(t)$ are respectively the i^{th} and the j^{th} $(1 \le i, j \le N)$ row of $\mathbf{x}(t)$, $R_{s_i^* s_j}(\tau) = |E_k|^2 e^{jw_k t}$, and $R_{n_i^* n_j}(\tau) = 0$. For the T_p pseudosnapshots, the pseudodata matrix is defined as

$$\mathbf{G} = \left\{ \begin{bmatrix} \mathbf{g}_x(\tau) \\ \mathbf{g}_x^*(-\tau) \end{bmatrix} | \tau = n_p P_s,\ n_p = 1, \ldots, T_P \right\}, \quad (3)$$

where P_s is the pseudosampling period that satisfies the Nyquist sampling theorem. For convenience, let the 1st sensor be the reference, $\mathbf{g}_x(\tau) = [R_{x_1^* x_1}(\tau), R_{x_1^* x_2}(\tau), \ldots, R_{x_1^* x_N}(\tau)]^T$. Then, the covariance matrix of $\mathbf{G}$ is calculated as

$$\mathbf{R}_G = E\left[\mathbf{G}\mathbf{G}^H\right] \approx \frac{1}{T_p} \sum_{n_p=1}^{T_p} \mathbf{g}\left(n_p P_s\right)\mathbf{g}^H\left(n_p P_s\right). \quad (4)$$

Vectorizing $\mathbf{R}_G$ yields

$$\mathbf{r}_G = \mathrm{vec}\left(\mathbf{R}_G\right) = \mathbf{B}\mathbf{z}, \quad (5)$$

where $\mathbf{z} = [|E_1|^4, |E_2|^4, \ldots, |E_K|^4]^T$ and the k^{th} column of $\mathbf{B}$ can be denoted as

$$\tilde{\mathbf{a}}(\theta_k) = \begin{bmatrix} \mathbf{a}(\theta_k) \otimes \mathbf{a}^*(\theta_k) \\ \mathbf{a}(\theta_k) \otimes \mathbf{a}(\theta_k) \\ \mathbf{a}^*(\theta_k) \otimes \mathbf{a}^*(\theta_k) \\ \mathbf{a}^*(\theta_k) \otimes \mathbf{a}(\theta_k) \end{bmatrix}, \quad (6)$$

where the term $\tilde{\mathbf{a}}(\theta_k)$ in (6) behaves like a virtual steering vector of a longer virtual ULA. More specifically, the union of $\mathbf{a}(\theta_k) \otimes \mathbf{a}^*(\theta_k)$ and $\mathbf{a}^*(\theta_k) \otimes \mathbf{a}(\theta_k)$ is respectively corresponding to DCA and its mirror version; $\mathbf{a}(\theta_k) \otimes \mathbf{a}(\theta_k)$ and $\mathbf{a}^*(\theta_k) \otimes \mathbf{a}^*(\theta_k)$ are respectively corresponding to SCA and its mirror version. Then, the spatial smoothing MUSIC or sparse construction approach can be performed for underdetermined DOA estimation, and the above procedure is termed as the vectorized conjugate augmented MUSIC (VCAM) [17].

3. Low Coarray Redundancy Array Configuration

Definition 1. Assume $2 < N_1 \le N_2$, $N_1 \in \mathbf{Z}^+$, and $N_2 \in \mathbf{Z}^+$, after normalizing by d, the configuration of the proposed array with $N = N_1 + N_2$ antenna elements is defined by

$$\begin{cases} \mathbb{L} = \mathbb{L}_1 \cup \mathbb{L}_2, \\ \mathbb{L}_1 = 1 + (l-1)N_1, \quad l \in \mathbb{Z}(N_1), \\ \mathbb{L}_2 = N_1^2 - N_1 + N_2 + l, \quad l \in \mathbb{Z}(N_2). \end{cases} \quad (7)$$

Intuitively, an example of $N_1 = N_2 = 3$ is given in Figure 1, where white circles and black circles denote the sensor locations of subarray $\mathbb{L}_1$ and $\mathbb{L}_2$, respectively.

From the perspective of coarray equivalence, the proposed array, NA, and TNA are compared in Figure 2 with the number of antenna elements being $N = 6$, where the red circles and blue triangles indicate the virtual sensors in DCA and SCA, respectively, and black crosses indicate holes. Note that the DCA, SCA, and SDCA are origin-symmetric, here the nonnegative parts of the abovementioned coarrays are selected for performance comparison, which are respectively abbreviated as n-DCA, n-SCA, and n-SDCA. The sensors in the rectangular dashed box indicate the overlapping virtual sensors between the n-DCA and the consecutive n-SCA. We can see from Figure 2 that the n-SDCA is continuous in the range of (0, 24) for the proposed array, while (0, 16) for NA and (0, 22) for TNA. Moreover, there exists only 1 overlapping virtual sensor for the proposed array, while 10 for NA and 4 for TNA.

Proposition 1. *Some properties of the proposed array configuration in the virtual coarray are listed as follows:*

(i) The DCA of the proposed array is continuous in set of $\mathbb{Z}(-S_1) \cup \mathbb{Z}(0) \cup \mathbb{Z}(S_1)$ *with* $S_1 = N_1^2 - N_1 + 2N_2 - 1$

(ii) The SCA of the proposed array is continuous in set of $\{¢(S_3) - ¢(S_2)\} \cup \{¢(-S_3) - ¢(-S_2)\}$ *with* $S_3 = 2(N_1^2 - N_1 + 2N_2)$, *let* $\varepsilon = N_2 - N_1 \in ¢$, *and the value of* S_2 *is given as follows:*

(a) if $0 \le \varepsilon < 2$, $S_2 = N_1^2 + 2$

(b) if $\varepsilon = 2$ *or* 3, $S_2 = N_1^2 - N_1 + N_2 + 2$

(c) if $\varepsilon \ge 4$, $S_2 = \begin{cases} N_1^2 + N_1 + 2, & N_1 = \varepsilon - 1, \\ N_1^2 - N_1 + N_2 + 2, & \text{else} \end{cases}$

Proof. See Appendix A. □

Proposition 2. *The proposed array has hole-free DCA and SDCA, and the maximum consecutive DOF is* $4(N_1^2 - N_1 + 2N_2) + 1$.

Proof. See Appendix B. Note that for a sparse array configuration with the fixed number of antenna elements, the higher consecutive DOF means larger virtual array aperture and more accurate DOA estimation. Therefore, it is essential to look for appropriate N_1 and N_2 to maximize the consecutive DOF. □

Corollary 1. *After optimizing* N_1 *and* N_2, *the optimal consecutive DOF and the corresponding solutions are given as*

$$\mathrm{DOF}_{\max} = \begin{cases} (N+1)^2, & \text{if } N_1 = N_2 = \dfrac{N}{2}, \\ N^2 + 8, & \text{if } N_1 = \dfrac{N-1}{2}, N_2 = \dfrac{N+1}{2}. \end{cases} \quad (8)$$

Proof. The optimal DOF under the constraint of $N = N_1 + N_2$ can be cast as the following optimization problem:

$$\max_{N_1, N_2} \mathrm{DOF} = 4\left(N_1^2 - N_1 + 2N_2\right) + 1 \quad \text{s.t.} N = N_1 + N_2. \quad (9)$$

Using arithmetic mean-geometric mean (AM-GM) inequalities, the solutions are obtained from (8). According to the above analysis, the proposed array exhibits the advantages in terms of consecutive DOF and virtual array aperture. From the view of coarray efficiency, the overlapping

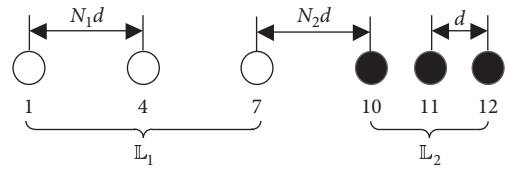

FIGURE 1: An example of the proposed array configuration with $N_1 = N_2 = 3$.

FIGURE 2: Virtual coarrays of the proposed array and NA with $N = 6$, (a) NA, (b) TNA, and (c) the proposed array.

virtual sensors between the DCA and SCA lead to coarray redundancy, which, to some extent, reduce the number of available virtual coarrays. In view of this, the concept of CRR is introduced to evaluate the coarray overlap. □

Definition 2. CRR denotes the ratio of the overlapping virtual sensors between the DCA and SCA, which is given by

$$\kappa = \frac{2(S_1 - S_2 + 1)}{(2S_3 + 1)}. \tag{10}$$

More specifically, CRR of the proposed array configuration can be calculated as

$$\text{if } 0 \le \varepsilon < 2, \quad \kappa = \frac{4N_2 - 2N_1 - 4}{4\left(N_1^2 - N_1 + 2N_2\right) + 1},$$

$$\text{if } \varepsilon = 2 \text{ or } 3, \quad \kappa = \frac{2N_2 - 4}{4\left(N_1^2 - N_1 + 2N_2\right) + 1},$$

$$\text{if } \varepsilon \ge 4, \quad \kappa = \begin{cases} \dfrac{4N_1}{4\left(N_1^2 - N_1 + 2N_2\right) + 1}, & N_1 = \varepsilon - 1, \\ \dfrac{2N_2 - 4}{4\left(N_1^2 - N_1 + 2N_2\right) + 1}, & \text{else.} \end{cases} \tag{11}$$

Proposition 3. *For the optimal DOF given in Corollary 1, if $N_1 = N_2 = (N/2) > 2$, the corresponding CRR is no more than 0.0496; if $N_2 = (N + 1/2) > N_1 = (N - 1/2) > 2$, the corresponding CRR is no more than 0.1053.*

Proof. If $N_1 = N_2 = (N/2) > 2$, the corresponding CRR can be simplified to $\kappa = (4N_2 - 2N_1 - 4/4(N_1^2 - N_1 + 2N_2) + 1) = (N - 4/(N + 1)^2)$. Then, the first-order derivative of κ is taken as $(\partial\kappa/\partial N) = (9 - N/(N + 1)^3)$. Since N is even, the maximum of κ is calculated as $\kappa_{\max} = \max(\kappa_{N=8}, \kappa_{N=10}) = 0.0496$. If $N_2 = N + 1/2$, $N_1 = N - 1/2$, the corresponding CRR can be simplified to $\kappa = (4N_2 - 2N_1 - 4/4(N_1^2 - N_1 + 2N_2) + 1) = (N - 1/N^2 + 8)$. Similarly, the first-order derivative of κ is taken as $\partial\kappa/\partial N = (-N^2 + 2N + 8/(N^2 + 8)^2)$. Note that N is odd; the maximum of κ is calculated as $\kappa_{\max} = \max(\kappa_{N=7}) = 0.1053$. □

4. Numerical Simulations

In this section, numerical simulations have been carried out to evaluate the performance of the proposed array, where SdNA [18] and TNA [21] are selected for performance comparison. In the first simulation, the CRR scatters versus $\varepsilon = N_2 - N_1$ are plotted in Figure 3, and the blue asterisks indicate the case where N is even and the red squares indicate the case where N is odd. It can be observed that the CRR of the proposed array tends to increase with the increase of ε, thus the optimal CRR can be obtained from $\varepsilon = 0$ when N is even and $\varepsilon = 1$ when N is odd.

In the second simulation, the CRR of three array configurations with $\varepsilon = 0$ and $\varepsilon = 1$ are respectively compared in Figures 4 and 5. The results show that the proposed array can achieve the smallest CRR compared to SdNA and TNA with the same number of antenna elements. Also, it has been concluded that the CRR of the proposed array is no more than 0.0496 when N is even and no more than 0.1053 when N is odd, which has been verified in Proposition 3.

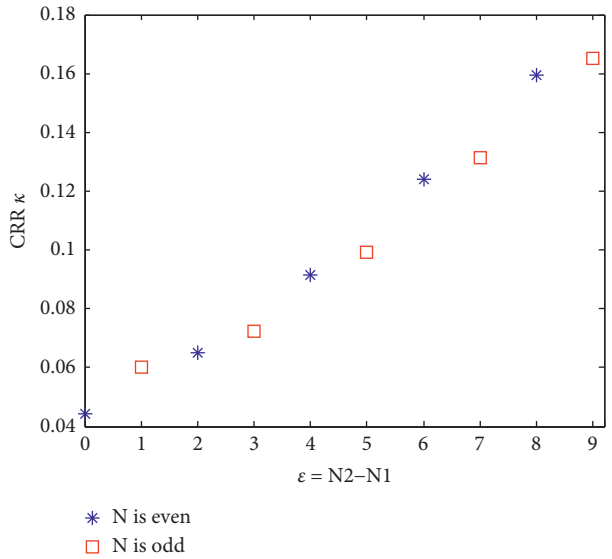

Figure 3: The scatter plot of CRR.

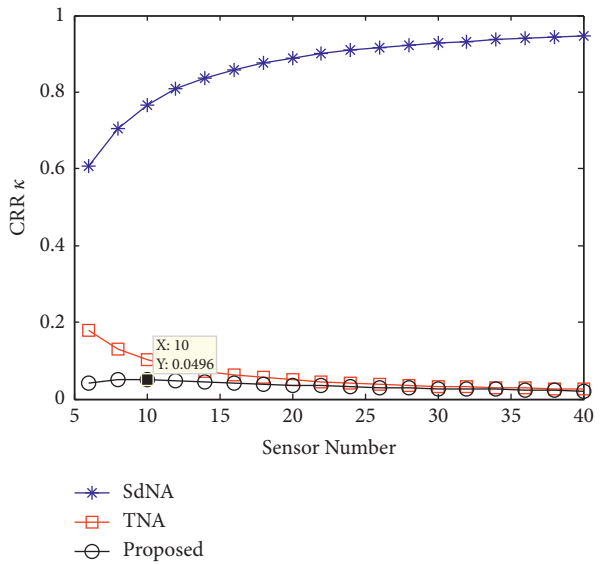

Figure 4: Comparison of CRR with different sensor number ($\varepsilon = 0$).

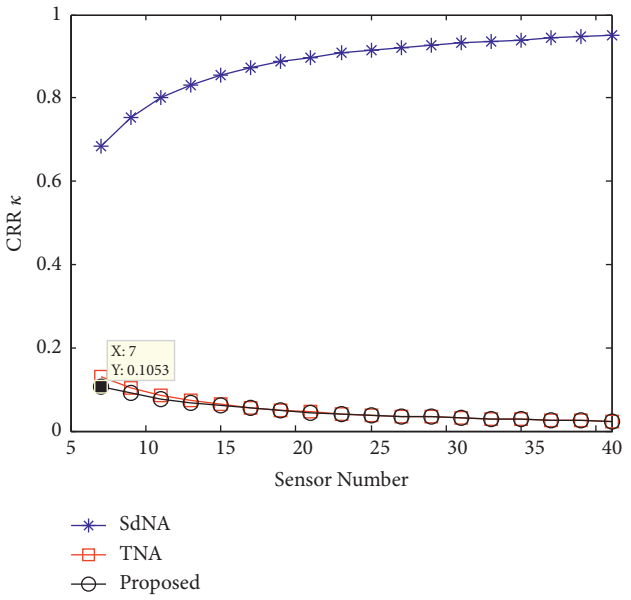

Figure 5: Comparison of CRR with different sensor number ($\varepsilon = 1$).

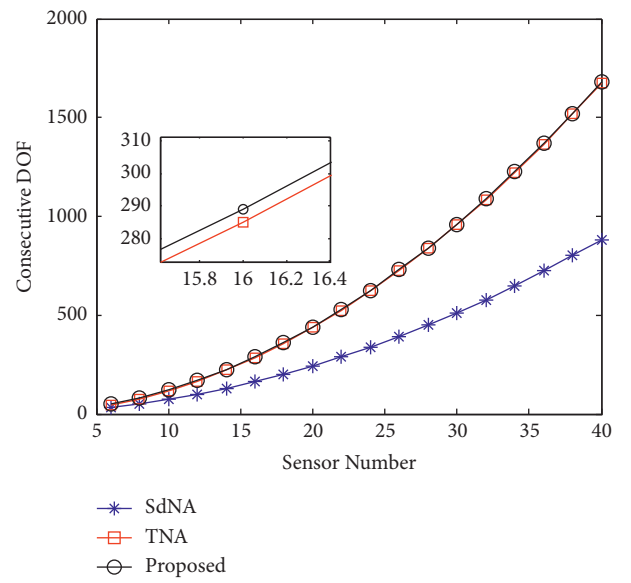

Figure 6: Comparison of consecutive DOF.

In the third simulation, we compare the consecutive DOF of three array configurations and the simulation results are depicted in Figure 6. As can be seen from Figure 6, the proposed array can obtain more consecutive DOF than the other two arrays benefitting from the lower CRR. This implies that there exist few overlapping sensors between the DCA and SCA of the proposed array, thus more effective virtual sensors can be utilized for the construction of SDCA.

Then, the DOA estimation performance is investigated in the last simulation. We consider $K = 27$ narrowband sources uniformly distributed between -60° and 60° impinging on the proposed sparse array with 8 sensors, where SNR being 0 dB and $T_s = T_p = 200$. Figure 7 depicts the MUSIC spectrum of the proposed array where the blue solid lines denote the angle estimates and the red dotted lines denote the incident sources. It can be seen that the proposed array can detect 27 impinging sources with only 8 sensors, and the estimated spectrum has sharp and clearly discernible peaks in the vicinity of the true impinging sources.

Figures 8 and 9 respectively depict the root mean square error (RMSE) of DOA estimation versus SNR and snapshots via 200 Monte Carlo trials, where RMSE is defined as

$$\text{RMSE} = \sqrt{\frac{1}{200K}\sum_{n=1}^{200}\sum_{k=1}^{K}\left(\hat{\theta}_{n,k} - \theta_{n,k}\right)^2}, \tag{12}$$

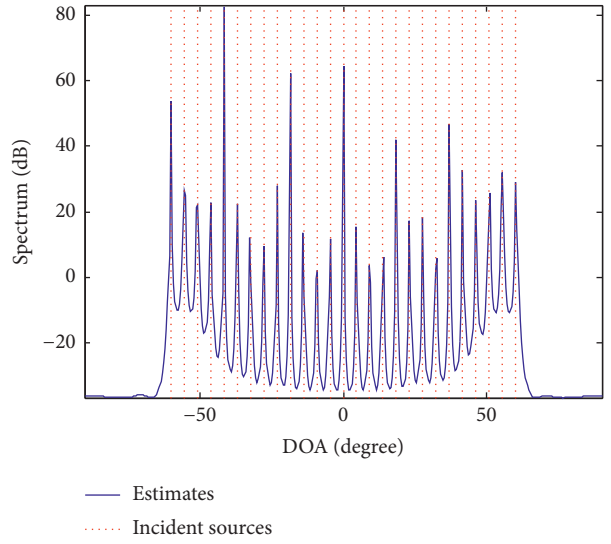

Figure 7: The MUSIC spectrum of the proposed array with $N = 8$.

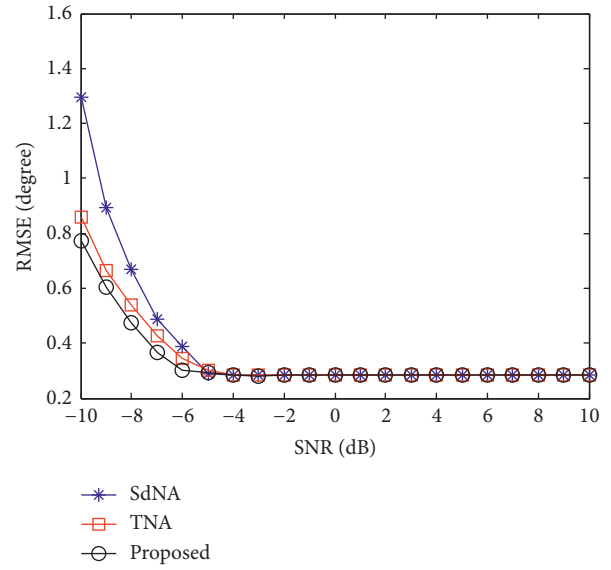

Figure 8: Comparison of DOA estimation performance (RMSE versus SNR).

with $\hat{\theta}_{n,k}$ being the estimate of the kth impinging source for the nth Monte Carlo trial. All the simulation conditions are the same as Figure 7, except that the snapshot number is fixed at 200 in Figure 8 and the SNR is fixed at −6 dB in Figure 9. The results show that the proposed array is superior to the other two array configurations in terms of DOA estimation accuracy, which mainly attributed to the larger consecutive DOF and the lower CRR of the proposed array.

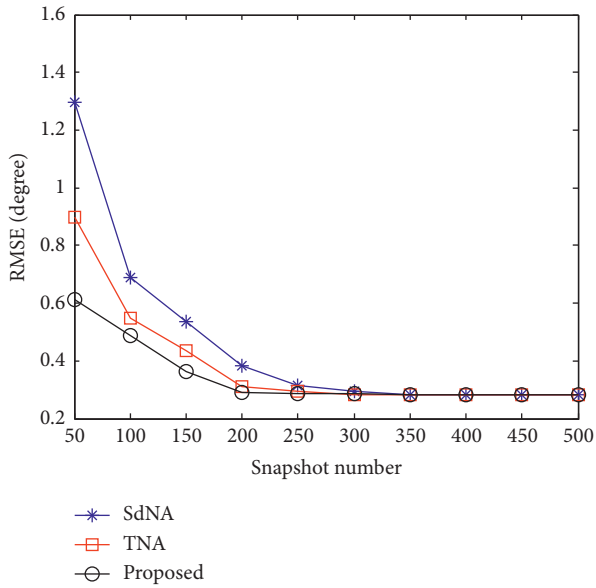

Figure 9: Comparison of DOA estimation performance (RMSE versus snapshots).

5. Conclusions

This paper presents a novel sparse array configuration for accurate DOA estimation, which has fewer coarray overlapping sensors and more consecutive DOF as compared with most of the existing sparse array configurations. From the perspective of coarray equivalence, the proposed array has hole-free DCA and SDCA. The closed-form CRR expressions of the proposed array are derived in order to evaluate the coarray overlap quantitatively. With the utilization of the proposed array, the VCAM approach is adopted for DOA estimation. The results of the theoretical analysis and the numerical simulations demonstrate the effectiveness and favorable performance of the proposed array configuration and DOA estimation performance.

Appendix

A. Proof of Proposition 1

(i) The positive part of the difference set between $\mathbf{L}_1$ and $\mathbf{L}_2$ is $\{\mathbf{L}_2 - \mathbf{L}_1\}$, which distributes continuously in the set of $\{\mathbb{Z}(S_1) - \mathbb{Z}(N_2)\}$ with $S_1 = N_1^2 - N_1 + 2N_2 - 1$. Similarly, the positive part of $\{\mathbf{L}_2 - \mathbf{L}_2\}$ is continuous in the set of $\{\mathbb{Z}(0) \cup \mathbb{Z}(N_2 - 1)\}$. Thus, the whole DCA (containing both the positive part and the negative part) of the proposed array is hole-free, which is continuous in the set of $\{\mathbb{Z}(-S_1) \cup \mathbb{Z}(0) \cup \mathbb{Z}(S_1)\}$.

(ii) The positive part of the sum set $\{\mathbf{L}_1 + \mathbf{L}_2\}$ is continuous in the set of $\{\mathbb{Z}(2N_1^2 - 2N_1 + 2N_2 + 1) - \mathbb{Z}(N_1^2 - N_1 + N_2 + 2)\}$ and $\{\mathbf{L}_2 + \mathbf{L}_2\}$ is also continuous in the set $\{\mathbb{Z}(S_3) - \mathbb{Z}(2N_1^2 - 2N_1 + 2N_2 + 2)\}$ with $S_3 = 2(N_1^2 - N_1 + 2N_2)$. Thus, the positive set of $\{(\mathbf{L}_1 + \mathbf{L}_2) \cup (\mathbf{L}_2 + \mathbf{L}_2)\}$ is continuous in the set $\{\mathbb{Z}(S_3) - \mathbb{Z}(N_1^2 - N_1 + N_2 + 2)\}$. By contrast, the set $\{\mathbf{L}_1 + \mathbf{L}_1\}$ is a discontinuous set composed of discrete points which are directly determined by N_1 and ε. More specifically, if $0 \le \varepsilon < 2$, the largest element in $\{\mathbf{L}_1 + \mathbf{L}_1\}$ is $N_1^2 + 2$, where $N_1^2 - N_1 + N_2 + 2 = N_1^2 + 2$ when $\varepsilon = 0$ and $N_1^2 - N_1 + N_2 + 2 - (N_1^2 + 2) = 1$ when $\varepsilon = 1$. Then, the positive SCA can be written as $\{\mathbb{Z}(S_3) - \mathbb{Z}(S_2)\}$ with $S_2 = N_1^2 + 2$ in the case of $0 \le \varepsilon < 2$. If $\varepsilon = 2$ or 3, the largest element in $\{\mathbf{L}_1 + \mathbf{L}_1\}$ is $N_1^2 - N_1 + N_2 + 2$, which means the positive SCA is $\{\mathbb{Z}(S_3) - \mathbb{Z}(S_2)\}$ with $S_2 = N_1^2 - N_1 + N_2 + 2$. If $\varepsilon \ge 4$ and $N_1 = \varepsilon - 1$, the largest element in $\{\mathbf{L}_1 + \mathbf{L}_1\}$ is $N_1^2 + N_1 + 2$ and $N_1^2 - N_1 + N_2 + 2 - (N_1^2 + N_1 + 2) = 1$, then the positive SCA is $\{\mathbb{Z}(S_3) - \mathbb{Z}(S_2)\}$ with $S_2 = N_1^2 + N_1 + 2$. If $\varepsilon \ge 4$ and $N_1 \ne \varepsilon - 1$, the largest element in $\{\mathbf{L}_1 + \mathbf{L}_1\}$ is $N_1^2 - N_1 + N_2 + 2$, the corresponding positive SCA is $\{\mathbb{Z}(S_3) - \mathbb{Z}(S_2)\}$ with $S_2 = N_1^2 - N_1 + N_2 + 2$. Since the negative SCA and the positive SCA are symmetrical about the zero, the whole SCA of the proposed array is continuous in set of $\{\mathbb{Z}(S_3) - \mathbb{Z}(S_2)\} \cup \{\mathbb{Z}(-S_3) - \mathbb{Z}(-S_2)\}$.

B. Proof of Proposition 2

Based on Proposition 1, the whole DCA is continuous in the set of $\{\mathbb{Z}(-S_1) \cup \mathbb{Z}(0) \cup \mathbb{Z}(S_1)\}$ with $S_1 = N_1^2 - N_1 + 2N_2 - 1$, which means the DCA of the proposed array is hole-free. Also, $S_2 = N_1^2 + 2$ holds in the case of $0 \le \varepsilon < 2$, then we have $S_1 - S_2 = 2N_2 - N_1 - 3 \ge 0$ since $N_2 \ge N_1 > 2$ ($N_1 \in \mathbb{Z}^+$, $N_2 \in \mathbb{Z}^+$). This implies that S_2 falls within the continuous interval of DCA; as a result, the SDCA is hole-free. Similar analyses can be utilized for the cases of $\varepsilon = 2$ or 3, $\varepsilon \ge 4$, i.e., if $\varepsilon = 2$ or $\varepsilon = 3$, $S_1 - S_2 = N_2 - 3 \ge 0$; if $\varepsilon \ge 4$ and $N_1 = \varepsilon - 1$, $S_1 - S_2 = 2N_2 - 2N_1 - 3 \ge 5$; if $\varepsilon \ge 4$ and $N_1 \ne \varepsilon - 1$, $S_1 - S_2 = N_2 - 3 \ge 4$. Consequently, the SDCA of the proposed array is continuous in the set of $\{\mathbb{Z}(-S_1) \cup \mathbb{Z}(0) \cup \mathbb{Z}(S_1)\} \cup \{\mathbb{Z}(S_3) - \mathbb{Z}(S_2)\} \cup \{\mathbb{Z}(-S_3) - \mathbb{Z}(-S_2)\}$ and can be simplified to $\mathbb{Z}(-S_3) \cup \mathbb{Z}(0) \cup \mathbb{Z}(S_3)$, which means the proposed array has hole-free SDCA. Accordingly, the maximum consecutive DOF is $2S_3 + 1 = 4(N_1^2 - N_1 + 2N_2) + 1$.

Data Availability

No data were used in this study.

Conflicts of Interest

The authors declare that there are no conflicts of interest regarding the publication of this paper.

Acknowledgments

This work was supported by the National Natural Science Foundation of China under Grant no. 62101223 and Major Basic Research Project of the Natural Science Foundation of the Jiangsu Higher Education Institutions of China under Grant nos. 20KJB510027 and 20KJA510008.

References

[1] H. Wang, X. Li, R. H. Jhaveri et al., "Sparse bayesian learning based channel estimation in FBMC/OQAM industrial IoT networks," *Computer Communications*, vol. 176, pp. 40–45, 2021.

[2] M. Agatonović, Z. Stanković, and N. Dončov, "Application of artificial neural networks for efficient high-resolution 2D DOA estimation," *Radio Engineering*, vol. 21, no. 4, pp. 1178–1186, 2012.

[3] H. Krim and M. Viberg, "Two decades of array signal processing research: the parametric approach," *IEEE Signal Processing Magazine*, vol. 13, no. 4, pp. 67–94, 1996.

[4] L. Wan, Y. Sun, L. Sun, Z. Ning, and J. J. P. C. Rodrigues, "Deep learning based autonomous vehicle super resolution DOA estimation for safety driving," *IEEE Transactions on Intelligent Transportation Systems*, vol. 22, no. 7, pp. 4301–4315, 2021.

[5] S. Qin, Y. D. Zhang, and M. G. Amin, "Improved two-dimensional DOA estimation using parallel coprime arrays," *Signal Processing*, vol. 172, Article ID 107428, 2020.

[6] W. Zheng, X. Zhang, Y. Wang, J. Shen, and B. Champagne, "Padded coprime arrays for improved DOA estimation: exploiting hole representation and filling strategies," *IEEE Transactions on Signal Processing*, vol. 68, pp. 4597–4611, 2020.

[7] R. Cohen and Y. C. Eldar, "Sparse array design via fractal geometries," *IEEE Transactions on Signal Processing*, vol. 68, pp. 4797–4812, 2020.

[8] G. Qin, M. G. Amin, and Y. D. Zhang, "DOA estimation exploiting sparse array motions," *IEEE Transactions on Signal Processing*, vol. 67, no. 11, pp. 3013–3027, 2019.

[9] P. P. Vaidyanathan and P. Pal, "Sparse sensing with co-prime samplers and arrays," *IEEE Transactions on Signal Processing*, vol. 59, no. 2, pp. 573–586, 2011.

[10] P. Pal and P. P. Vaidyanathan, "Nested arrays: a novel approach to array processing with enhanced degrees of freedom," *IEEE Transactions on Signal Processing*, vol. 58, no. 8, pp. 4167–4181, 2010.

[11] S. Qin, Y. D. Zhang, and M. G. Amin, "Generalized coprime array configurations for direction-of-arrival estimation," *IEEE Transactions on Signal Processing*, vol. 63, no. 6, pp. 1377–1390, 2015.

[12] A. Raza, W. Liu, and Q. Shen, "Thinned coprime array for second-order difference co-array generation with reduced mutual coupling," *IEEE Transactions on Signal Processing*, vol. 67, no. 8, pp. 2052–2065, 2019.

[13] C.-L. Liu and P. P. Vaidyanathan, "Super nested arrays: linear sparse arrays with reduced mutual coupling-part I: Fundamentals," *IEEE Transactions on Signal Processing*, vol. 64, no. 15, pp. 3997–4012, 2016.

[14] J. Liu, Y. Zhang, Y. Lu, S. Ren, and S. Cao, "Augmented nested arrays with enhanced DOF and reduced mutual coupling," *IEEE Transactions on Signal Processing*, vol. 65, no. 21, pp. 5549–5563, 2017.

[15] H. Wang, L. Xu, Z. Yan, and T. A. Gulliver, "Low-complexity MIMO-FBMC sparse channel parameter estimation for industrial big data communications," *IEEE Transactions on Industrial Informatics*, vol. 17, no. 5, pp. 3422–3430, 2021.

[16] L. Wan, K. Liu, Y.-C. Liang, and T. Zhu, "DOA and polarization estimation for non-circular signals in 3-D millimeter wave polarized massive MIMO systems," *IEEE Transactions on Wireless Communications*, vol. 20, no. 5, pp. 3152–3167, 2021.

[17] X. Wang, Z. Chen, S. Ren, and S. Cao, "DOA estimation based on the difference and sum coarray for coprime arrays," *Digital Signal Processing*, vol. 69, pp. 22–31, 2017.

[18] Z. Chen, Y. Ding, S. Ren, and Z. Chen, "A novel nested configuration based on the difference and sum co-array concept," *Sensors*, vol. 18, no. 9, pp. 1–17, 2018.

[19] W. Si, Z. Peng, C. Hou, and F. Zeng, "Improved nested arrays with sum-difference coarray for DOA estimation," *IEEE Sensors Journal*, vol. 19, no. 16, pp. 6986–6997, 2019.

[20] P. Zhao, K. Wang, G. Hu, and L. Wan, "Underdetermined DOA estimation using unfold coprime array from the perspective of sum-difference co-array," *IEEE Access*, vol. 7, pp. 168557–168564, 2019.

[21] Y. Wang, W. Wu, X. Zhang, and W. Zheng, "Transformed nested array designed for DOA estimation of non-circular signals: reduced sum-difference co-array redundancy perspective," *IEEE Communications Letters*, vol. 24, no. 6, pp. 1262–1265, 2020.

[22] F. Izedi, M. Karimi, and M. Derakhtian, "Joint DOA estimation and source number detection for arrays with arbitrary geometry," *Signal Processing*, vol. 140, pp. 149–160, 2017.